Proceedings of ERAD (2002): 161–166 © Copernicus GmbH 2002

ERAD 2002

Deriving water cloud properties from vertical pointing 95 GHz Doppler radar

J. Meywerk[1], **O. Sievers**[1], **M. Quante**[1], **V. Venema**[2], **and S. Crewell**[2]

[1]GKSS Research Center, Institute for Coastal Research, Geesthacht, Germany
[2]University of Bonn, Meteorological Institute, Bonn, Germany

Abstract. During the main observational phase of 4D-CLOUDS, conducted at Cabauw, The Netherlands, from 1 August through 31 September 2001, cloud radar parameters like reflectivity, linear depolarization ratio and Doppler velocities have been observed using a 95 GHz cloud radar. These datasets, together with other remotely sensed parameters from the ground and in situ airborne measurements, will be used to derive properties of water clouds used by radiation codes of dynamical atmospheric models to develop enhanced cloud parameterization schemes.

The above mentioned radar data sets have been taken with vertically pointing antenna. Simultaneously a multi-channel passive microwave radiometer and a lidar ceilometer were operated close to the radar. Corrections due to atmospheric absorption (gaseous) and attenuation due to clouds (mainly loss of signal due to scattering) had to be applied to the data. Also an attempt has been made to distinguish between drizzle containing and drizzle free water clouds. The corrections will be discussed in detail and have been applied to the radar reflectivity profiles. After the liquid water content is being calculated (for a fixed liquid water path) the maximum in liquid water content of the cloud is increased by about 14% and shifted upward within the cloud. The applied corrections bring the liquid water profile closer to adiabatic in the middle and upper part of the cloud. Examples of corrected vertical profiles will be shown and discussed together with accompanying data sets from microwave radiometer and ceilometer.

1 Introduction

Even though only a tiny amount of total water available on Earth is (temporarily) stored in clouds, they play a major role in climate and weather on a wide range of spatial and temporal scales, mostly through their ability of changing the radiation budget at the surface and of the atmosphere and redistribution of heat and moisture vertically and spatially. The impact of clouds on climate and climate change on a regional and global scale is only poorly understood. The most challenging aspect is their high temporal and spatial variability, as well as the high variability of their microphysical properties. Atmospheric models can neither resolve clouds nor their internal variability below their spatial resolution, even though sub-grid scale properties can have a large impact on the energy budget of the surface and the overlying atmosphere. Hence, parameterizations for those sub-grid cloud processes need to be applied. The cloud parameterizations in atmospheric models, however, are not sufficient, leading to large errors in heating and cooling rates which couple back to the dynamics. To overcome some of these shortcomings described above, the 4D-CLOUDS (http://www.meteo.uni-bonn.de/projekte/4d-clouds/) project seeks to improve these parameterizations of low level water clouds by first characterizing radiation relevant cloud micro- and macro-physical parameters, such as liquid water path, liquid water content, droplet size spectra, their lower and upper boundaries, to list the most important parameters. Typical patterns in time and space will be extracted from the observational data. With the help of statistical analysis of measured cloud fields and their internal variability as well as large eddy simulation models, sub-grid scale clouds will be produced for which the three dimensional radiative transfer is investigated. From the calculations of realistic clouds it is expected to develop more realistic parameterizations for sub-grid scale water clouds in regional and global models.

One central parameter, which is used in atmospheric models to parameterize the radiative transfer is the liquid water profile of clouds, which will be derived in this study by combining a 95 Ghz radar, a passive microwave radiometer and a ceilometer. The data presented here originates from the joint field phase of the BALTEX Cloud Liquid Water Network (CLIWA-NET) (van Lammeren et al., 2001) and 4D-CLOUDS, which took place in Cabauw/Netherlands in August and September 2001.

Correspondence to: J. Meywerk (Jens.Meywerk@gkss.de)

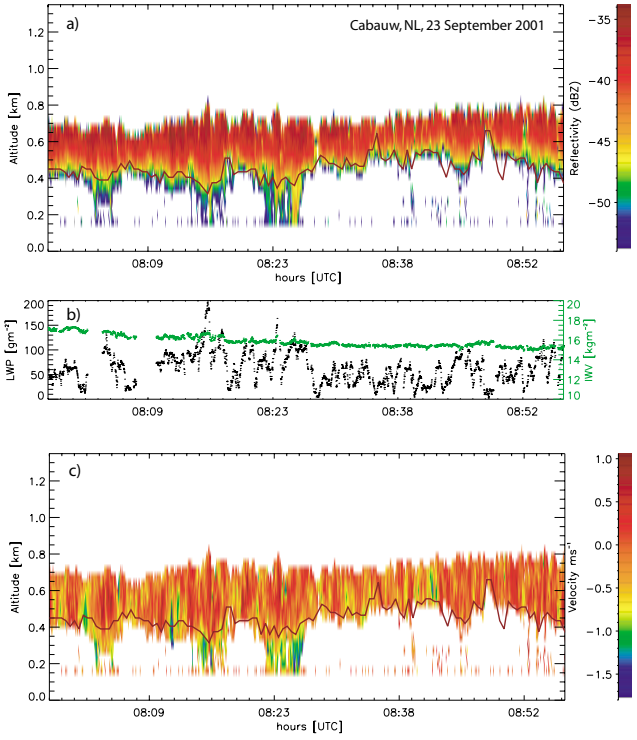

Fig. 1. Time series of **(a)** uncorrected radar reflectivities, **(b)** liquid water path and integrated water vapor as derived from passive microwave radiometer and **(c)** Doppler velocity from cloud radar as observed on 23 September 2001 between 7:57 and 8:57 UTC.

2 Equipment used

For this study we used a combination of three different instruments which operated side by side, simultaneously probing the same cloud volume (MIRACLE) and its associated column (MICCY), respectively.

The cloud radar used is the GKSS owned and operated 95 GHz polarimetric Doppler radar (MIRACLE). This W-band radar allows to detect the backscatter signal of most water clouds with typical droplet size distributions and number densities. Beside other parameters like pulse length, pulse repetition frequency and polarization, the vertical resolution can be selected between 7.5 m and 82.5 m. The narrow beam width of 0.17° leads to a horizontal resolution of about 30 m at a distance of 10 km if no wind is present. For windy conditions this resolution is decreased linearly with wind speed and averaging interval. With this capability it is possible to detect low level water clouds with a sufficient temporal and spatial resolution. The accuracy of the radar for averages of at least 0.1 seconds has been estimated to be about 2 dB, through direct intercomparison with a calibrated radar of the same kind. The threshold detection signal is set to −54 dBZ. A more detailed description of the radar system can be found in Quante et al. (2000). The advantages of being able to detect such weak cloud reflection signals due to the high frequency and the design of the instrument are traded against some disadvantages resulting from the frequency of the cloud radar that need to be accounted for. The relatively high frequency leads to

- attenuation due to cloud liquid water,
- gaseous absorption (water vapor and oxygen),
- relatively high far field condition,
- leaving the region in which the Rayleigh approximation is valid at relatively small particle sizes.

A passive microwave radiometer from University of Bonn (MICCY) measured atmospheric emission at 21.3, 23.8 and 31.7 GHz. With an appropriate calibration of the instrument (Hogg et al., 1983) it is possible to calculate the liquid water path (LWP) to an accuracy of 10–30% (Westwater, 1978). The beam width of the radiometer is 0.9° and the temporal resolution is 30 seconds.

As a third parameter, the ceilometer derived cloud base height from KNMI ceilometer was used to determine an estimate of the lower boundary of the cloud at visible wavelengths. The ceilometer used is the commercially available Vaisala CT75 lidar, which measures the backscatter at 905 nm wavelength. It has a vertical resolution of 15 m and a temporal resolution of 30 seconds. A more detailed description of the instrument and its operation can be found in Russchenberg et al. (1998) and will not be repeated here.

3 Estimating cloud liquid water profiles

In general there are several different ways to derive the liquid water profiles of low-level water clouds from ground based remotely sensed data. The easiest would be to simply apply a quadratic relationship between reflectivity and liquid water content, which has been developed for instance by Sauvageot and Omar (1987). This relationship was derived by calculating reflectivities from in situ airborne droplet size measurements and relating them to the calculated liquid water content.

Another more sophisticated approach was developed by Frisch et al. (1998) who used a combination of microwave radiometer and cloud radar reflectivity profiles to derive the profiles of liquid water content. Assuming that the sixth moment of the size distribution is proportional to its third moment squared, and the number concentration of cloud particles is constant with height, they find a relationship between liquid water path (LWP), radar reflectivity and liquid water content (LWC), which is even independent of the calibration of the radar.

In this study we used the LWC retrieval for non precipitating water cloud, based on the Frisch et al. (1998) algorithm, but with necessary corrections due to gaseous absorption and attenuation due to cloud liquid water before the algorithm is applied. Figure 1 shows the time series of uncorrected reflectivity and vertical velocity we used for this study. Figures 1a and 1c represent 5s averages of radar reflectivities and Doppler velocities with a vertical resolution

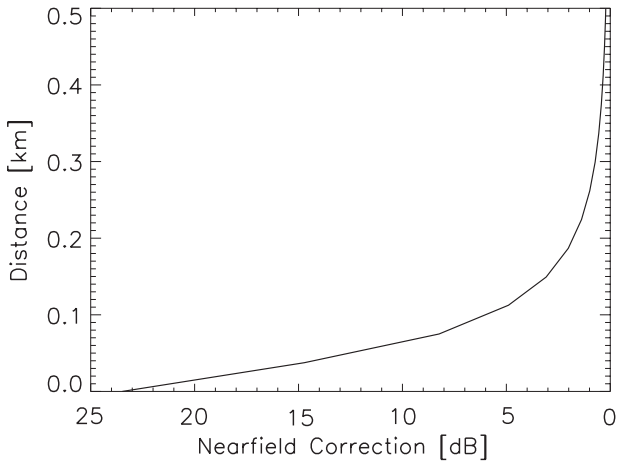

Fig. 2. Near field correction for MIRACLE.

of 37.5 m. The data was taken during the joint 4D-CLOUDS and CLIWA-NET field campaign at Cabauw, the Netherlands on 23 September 2001. During the entire morning until about noon, a stratocumulus layer was observed underneath a weak humidity inversion, which had a vertical extension of about 300m, with in general increasing altitude and decreasing thickness with time. From radar as well as airborne observation there were no cloud layers observed above this stratocumulus deck for the entire morning. The freezing level was at about 2 km altitude, well above the cloud layer, so the entire cloud can safely be considered a pure water cloud. The upper panel of Fig. 1a shows the reflectivity as recorded, after applying a cloud mask. The cloud mask is described in detail in Sievers et al. (this issue) and will not be repeated here. Reflectivities in general are increasing with altitude, with maximum values in the upper third of the cloud layer. The horizontal solid line is the lower cloud boundary as indicated by the ceilometer. It can be seen that for most of the time the radar detected lower boundary is close to the lower boundary 'seen' by the ceilometer. For some cases, however, there is considerable disagreement between both estimates. This is caused by drizzle drops (diameter between 50 and 400 μm) which leave the lower boundary of the cloud and evaporate on their way down, so never reaching the surface as precipitation. Since radar reflectivity is proportional to the 6th power of drop diameter a very small number of drizzle sized drops produce a detectable back scattering signal. The backscattering signal in the visible to near infrared wavelengths (as detected by the ceilometer) on the other hand, increases only with the square of the droplet diameter. This is why the ceilometer does not detect those drizzle sized drops, if their number density is not high enough.

The latter exhibits a general problem with radar reflectivities if drizzle sized droplets are present. Despite their high backscatter signal drizzle sized drops are not adding significant amounts of liquid water (Fox and Illingworth, 1997), since their number density is very low. The panel just underneath the reflectivity in Fig. 1b is the time series of liquid water path (LWP) and integrated water vapor (IWV) as derived from the microwave radiometer MICCY. The variance in retrieved LWP is much stronger in the LWP signal than would be expected from examining the radar reflectivities alone. The IWV decreases during the morning hours from about 17.5 kg m^{-2} at to about 8:00 UTC to 15.5 kg m^{-2} at about 9:00 UTC. The lower panel shows the vertical velocity as derived from the Doppler signal processing. Most of the vertical velocities are scattered around 0 m s^{-1}, but at those times when the radar detected lower cloud boundary well below the ceilometer cloud boundary, much higher and negative (indicating falling) vertical velocities of up to -1.3 m s^{-1} can be observed. This is another indication for drizzle sized drops leaving the cloud. The terminal velocity of cloud droplets is in general a function of cloud droplet size distribution (Khvorostyanov and Curry, 2002). The ceilometer cloud boundary is also overlaid to the velocity data as solid line.

4 Corrections applied to radar reflectivities

4.1 Near field correction

The near field correction is necessary since the radar equation is only derived for the so-called antenna far field, which involved several assumptions about the antenna gain and pattern shape. This leads to the necessity to correct the received signal for this error as long as the considered range gate is below this far field threshold. For the correction we followed a suggestion of Sekelsky (2002). The far field starts for the MIRACLE at 933 m distance from the antenna as can be seen from

$$r_f \geq \frac{2 \cdot d^2}{\lambda}.$$

λ is the wavelength, d is the antenna diameter and r_f is the distance from the radar, from which on the radar equation can be used without near field corrections. For all range gates below r_f, the near field correction needs to be applied. Figure 2 shows the near field correction for the MIRACLE, which is valid in the distance range from 23 m to 933 m. For extremely close targets ($\sim$80 m) a correction of about 10 dB would necessary. This becomes especially important if low boundary layer clouds are observed. The near field correction for the case considered here is very small.

4.2 Atmospheric absorption

Even though atmospheric absorption is weak (but not zero!) at 95 GHz there is still a non-negligible absorption of water vapor and oxygen. Compared to 3, and 35 GHZ radar the absorption due to water vapor and oxygen is more than an order of magnitude stronger in the 95 GHz region. Following a somewhat lengthy empirical function to calculate water vapor and oxygen absorption given by Ulaby (1981) we applied the correction of the signal due to these two gases. The necessary temperature, pressure and water vapor density profiles

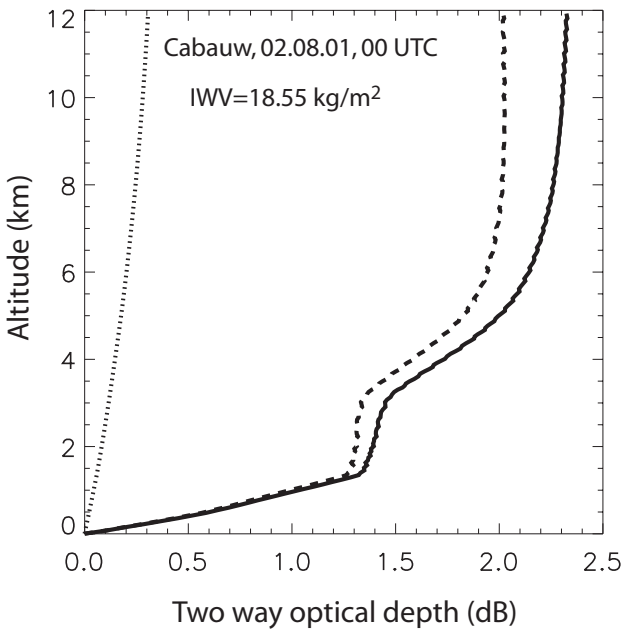

Fig. 3. Water vapor and oxygen two way optical depth calculated for 95 GHz for vertical pointing radar as a function of altitude (dotted: oxygen alone, dashed: water vapor alone, solid: combined effect).

were taken from the closest (in time and space) available radio sounding. Here we did not make use of MICCY derived temperature and humidity profiles, since we have been able to find a radio sounding which was started just 30 minutes before we started our measurements. From these profiles the water vapor as well as oxygen absorption coefficients have been calculated. An example of the magnitude of this correction is given in Fig. 3, which has been calculated for a vertical two way signal path (to and from the scattering volume). The dotted line is the correction that needs to be applied to the received radar signal due to oxygen absorption alone. The dashed line is for the water vapor absorption and the solid line for the combined effect. As can be seen from the graph, even for a medium humid atmosphere with an integrated water vapor content of about 18.5 kg m^{-2} a correction of up to 2.5 dBZ needs to be applied to the signal, even for a vertical pointing antenna. Nicely to see is a relatively dry layer between 1.2 and about 3 km, for which the two way optical depth due to water vapor is not increasing very much, while the optical depth due to oxygen is not effected. It is clear from these calculations that it is necessary to apply these corrections even for vertical pointing radar if the reflectivity signal is used to derive quantitative estimates of LWC.

4.3 Attenuation correction due to cloud liquid water

The attenuation correction regarding hydrometeors has been applied similar to the approach described by Löhnert et al. (2001) but with a different method for calculating the liquid water content. If the Rayleigh approximation holds (Ulaby, 1981), the absorption coefficient k_c can be calculated by

$$k_c = \frac{6\pi}{\lambda} \cdot Im(-K) \cdot q(Z, Q),$$

with

$$K = \frac{k^2 - 1}{k^2 - 2},$$

and k denoting the complex refractive index of water and λ being the wavelength of the radar. The liquid water content q is being calculated using the approach by Frisch et al. (1998), which basically spreads the total liquid water path Q derived from the passive microwave radiometer to the entire cloud column as detected by the radar, weighted by the reflectivity profile retrieved from the radar in the following manner:

$$q_n = \frac{Q \cdot \sqrt{Z_n}}{\sum_{n=1}^{N} \sqrt{Z_n} \cdot \Delta z_n}.$$

The index n denotes the respective range gate or level, N is the total number of range gates in the cloud column under consideration. Z_n is the reflectivity in the n-th range gate and Δz_n is the respective range gate spacing, which is a constant for all range gates in each profile. Assuming that Z in the lowest cloud layer (n = 1) is not attenuated by the cloud, the optical depth of that layer can be calculated using

$$\tau_n = \sum_{i=1}^{n} k_i \cdot \Delta z_i,$$

which is the optical depth integrated from the lowest layer (i = 1) up the layer considered ($i = n$). The corrected reflectivity of the second layer from below is then calculated using $Z_n^c = Z_n \cdot e^{2\tau_n}$ with the index c denoting the corrected radar reflectivity of the n-th layer. This can be done for all cloud layers from the bottom to the cloud top recursively.

5 Results

After applying all corrections mentioned above the liquid water content has been calculated for the entire cloud column. The effect of the various corrections on the liquid water content can be seen in Fig. 4. The vertical profile of liquid water content for an example profile at 8:16:35 UTC is displayed for the entire cloud column. Applying the algorithm of Frisch et al. (1998) to the uncorrected data we receive the dotted curve with the asterix symbols. After applying the correction due to atmospheric absorption we get the dashed line marked with diamonds. Only a very small change can be seen towards lightly higher liquid water content in the upper layers of the cloud. After applying the liquid water correction there is another increase in liquid water content towards the upper part of the cloud. The maximum in liquid water content is more pronounced, while LWC in the lower layers decreases slightly. This is due to the increasing underestimation of radar reflectivities with increasing cloud thickness for

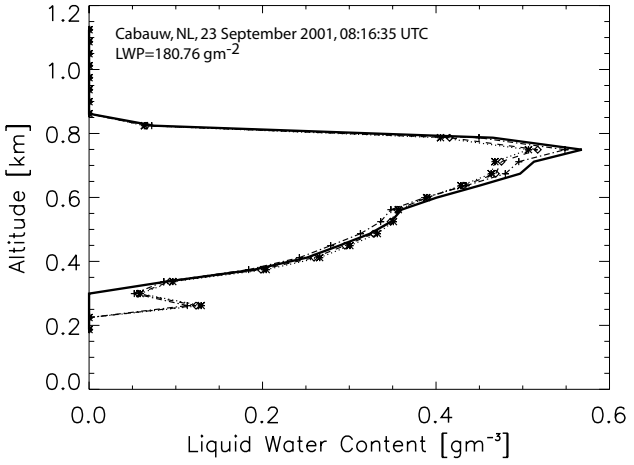

Fig. 4. Liquid water contend as calculated before any correction is applied (dotted with asterix) and after applying near field correction (dashed with diamonds), attenuation correction due to liquid water (dash-dotted with plus') and after rejection of drizzle underneath the cloud base (solid line), respectively. Example is calculated for 23 September 8:16:35 UTC.

uncorrected data. If we account for the drizzle underneath the cloud by cutting off all radar reflectivities underneath the ceilometer detected cloud base height, by assuming that the drizzle is not significantly adding liquid water to the scattering volume, we end up with the solid line, which basically redistributes all liquid water previously detected underneath the ceilometer cloud base height to the 'true' cloud starting at the ceilometer base height.

Figure 5 shows the time series of liquid water profiles for the uncorrected (a), the corrected (b), as well as the difference (c). Especially where the difference between ceilometer and radar derived lower cloud boundary is large a considerable increase in liquid water content in the upper part of the cloud can be observed; a direct result of the redistribution of all radar signal weighted LWP underneath the ceilometer cloud base. It is clearly seen from these plots that in general, for fixed liquid water path as dictated by using the Frisch (1998) algorithm, the liquid water content in the lower part of the cloud is shifted to higher levels, even more pronouncing the maximum liquid water content in the upper part of the cloud. It becomes clear that one must account for the corrections applied in this study if deriving physical quantities from the radar data.

During the same time in situ cloud observations have been done with an aircraft equipped with different cloud particle probes. At certain times the aircraft had been close to Cabauw, but never inside the same cloud volume as sensed by the radar. Since the spatial variability in cloud liquid water is extremely high there is no meaningful direct intercomparison possible for single data points. Thus, only the typical range of values and their variance in time and space can be compared. From the FSSP probes flown onboard the Merlin, the same morning in this cloud layer, cloud liquid water

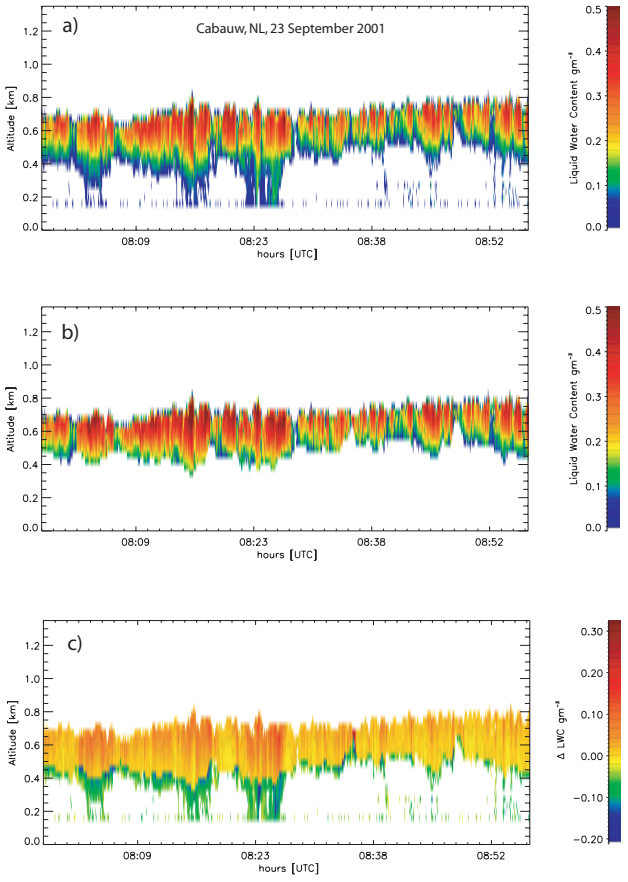

Fig. 5. Time series of liquid water path before **(a)** and after **(b)** applying corrections. **(c)** Exhibits the difference in LWC.

contents of the same magnitude of up to $0.5-0.6$ g m^{-3} have been found in the upper part of the clouds. Averaging times for these kind of data are typically about 10 seconds, representative for a 700 m long transect at an airspeed of 70 m s^{-1}. With an approximate wind speed of 5.7 m s^{-1} in the cloud layer (observed from radio soundings) this would translate to a 123 s average in the vertical pointing radar derived liquid water paths. Using these typical values an average of 25 successive profiles would be better comparable to the 700 m long horizontal transect of the cloud. Averaging in this way we receive a good agreement of ranges of liquid water paths as from the in situ data, suggesting that the remotely sensed liquid water path is close to the truth, if in situ observation is considered as truth. Considering the combined uncertainties resulting from the in situ measurement of LWC, the procedure used to derive the LWC from radar and the fact that the temporal and spatial variability in LWC is very high this result can be taken as very promising in retrieving LWC from ground base remote sensing technique.

When comparing LWC derived before and after applying all corrections we find that the gradient in LWC is increased from about 0.0012 to 0.0014 g m^{-3} m^{-1} in the upper and middle part of the cloud. The adiabatic LWC gradient is at 0.00153 g m^{-3} m^{-1} for the atmospheric profile and cloud ge-

ometry in this example, bringing the corrected profiles closer to adiabatic.

6 Conclusions and outlook

Is has been shown that using a combination of cloud radar, passive microwave radiometer and ceilometer we can and need to correct radar reflectivities for near field effects, gaseous absorption, and attenuation due to cloud liquid water itself, before using it to derive physical quantities such as liquid water profiles. If drizzle can be detected underneath the cloud it is also useful to reject these data when deriving cloud liquid water profiles, since drizzle "fakes" clouds in the radar reflectivities, but does at the same time not contribute substantially to the liquid water content.

The corrections applied here have been made under the following major assumptions:

- Clouds consist of pure water droplets at a fixed temperature.
- No significant amount of drizzle sized drops are inside the cloud.
- The 6th moment of droplet size distribution is proportional to their 3rd moment squared.
- The number density is constant with height.

These prerequisites have been ideally fulfilled for the dataset used in this study. The authors are aware, however, that the procedure described in this work is only applicable if the above mentioned assumptions are all fulfilled. Most important to make this procedure work for a wider range of situations would be to detect drizzle inside clouds and find out the drizzle impact on the radar reflectivity and subtract this part from the reflectivity before applying the procedure. If this can be achieved, liquid water content of even drizzle containing clouds could be estimated. Additional information like full Doppler velocity spectra (which were not available during this experiment due to technical limitations) could help determine the drizzle influence on the reflectivity signal.

In a next stage we will work on applying the above corrections to radar volume scans also taken quasi-simultaneous with the passive microwave radiometer during the same experiment. This approach, however, will not be as easy, since radar and microwave radiometer did not really scan the same volume at exactly the same time. Some kind of average liquid water path for each scan must be used for deriving liquid water contents for these scans, resulting in a somewhat smeared-out structure of liquid water inside the clouds. The data derived in this study will serve as input for 2D and 3D Monte Carlo radiative transport calculations.

References

Fox, N., A.J. Illingworth: The retrieval of stratocumulus cloud properties by ground-based cloud radar. J. Appl. Meteor., 36, 485–492, 1997.

Frisch, A.S., C.W. Fairall, G. Feingold, T. Utal, and J.B. Snider: On cloud radar microwave radiometer measurements of stratus cloud liquid water profiles. J. Geophys. Res., 103, No. D18, 23195–23197, 1998.

Hogg, D.C., F.O. Guiraud, J.B. Snider, M.T. Decker and E.R. Westwater: A steerable dual channel microwave radiometer for measurement of water vapor and liquid in the troposphere. J. Climate Appl. Meteor., 22, 789–806, 1983.

Khvorostyanov, V.I., and J.A. Curry: Terminal velocities of droplets and crystals: power laws with continuous parameters over the size spectrum. J. Atmos. Sci., 59, 1872–1884, 2002.

Löhnert, U., S. Crewell, and C. Simmer: Profiling cloud liquid water by combining active and passive microwave measurements with cloud model statistics. J. Atmos. Ocean. Tech., 18, 1354–1365, 2001.

Quante, M., H. Lemke, H. Flentje, P. Francis and J. Pelon: Boundaries and internal structure of mixed phase clouds as deduced from ground based 95 GHz radar and airborne lidar measurements. Phys. Chem. Earth (b), Vol. 25, No.10-12, 889–895, 2000.

Russchenberg, H., V. Venema, A. van Lammeren, A. Feijt, A. Apituley: Cloud measurements with lidar and 3GHz radar. Final report to ESA under ESTEC Contract No. PO 151912, ITCTR report: IRCTR-S-008-98, 42 pages, 1998.

Sauvageot, H. and J. Omar: Radar reflectivity of cumulus clouds. J. Atmos. Oceanic Technol., 4, 264–272, 1987.

Sekelsky, S.M.: Near-field reflectivity and antenna boresight gain corrections for millimeter-wave atmospheric radars. J. Atmos. Ocean. Tech., 19, 468–477, 2002.

Sievers, O., J. Meywerk, M. Quante: Statistics of non-precipitating daytime clouds, based on 95 GHz cloud radar measurements during BBC campaign. This issue, 2002.

Ulaby, F.T., R.K. Moore, and A. D. Fung: Microwave remote sensing, active and passive, Vol. 1, Artech House, 456pp, 1981.

Van Lammeren and the CLIWA-NET project team: The BALTEX BRIDGE Cloud Liquid Water Network Project: CLIWA-NET, Third Study Conference on BALTEX, Conference Proceedings, BALTEX Publication Series No. 20, July 2001, 239–240, 2001.

Westwater, E.R.: The accuracy of water vapor and cloud liquid water dertermination by dual-frequency ground-based microwave radiometry. Radio Sci., 13, 677–685, 1978.